Chapter 13

High-Overtone Bulk Acoustic Resonator

T. Baron, E. Lebrasseur, F. Bassignot, G. Martin, V. Pétrini and S. Ballandras

Additional information is available at the end of the chapter

http://dx.doi.org/10.5772/56175

1. Introduction

Piezoelectricity has been used for the development of numerous time&frequency passive devices [1]. Among all these, radio-frequency devices based on surface acoustic waves (SAW) or bulk acoustic waves (BAW) have received a very large interest for bandpass filter and frequency source applications. Billions of these components are spread each year around the world due to their specific functionalities and the maturity of their related technologies [2]. The demand for highly coupled high quality acoustic wave devices has generated a strong innovative activity, yielding the investigation of new device structures. A lot of work has been achieved exploiting thin piezoelectric films for the excitation and detection of BAW to develop low loss RF filters [3]. However, problems still exist for selecting the layer orientation to favor specific mode polarization and select propagation characteristics (velocity, coupling, temperature sensitivity, *etc*.). Moreover, for given applications, deposited films reveal incapable to reach the characteristics of monolithic substrates [4].

For practical implementation, BAW is applied for standard low frequency (5 to 10MHz) shear wave resonators on Quartz for instance. SAW, Film Bulk Acoustic Resonator (FBAR) and High overtone Bulk Acoustic Resonator (HBAR) devices are applied for standard radio-frequency ranges and more particularly in S band (2 to 4GHz). HBAR have been particularly developed along different approaches to take advantage of their extremely high quality factor and very compact structure. Until now, many investigations have been carried out using piezoelectric thin films (Aluminum Nitride – AlN, Zinc Oxide – ZnO) atop thick wafers of silicon or sapphire [5] but recent developments showed the interest of thinned single-crystal-based structure in that purpose [6]. Although marginal, their application has been mainly focused on filters and frequency stabilization (oscillator) purposes [7], but the demonstration of their effective implementation for sensor applications has been achieved recently [8]. These devices maximize the Q factor that can be obtained at room temperature using elastic waves, yielding quality factor times Frequency products ($Q.f$) close or slightly

above 10^{14}, *i.e.* effective *Q* factors of about 10,000 at 1GHz in theory (practically, *Q* factors in excess of 50,000 between 1.5 and 2GHz were experimentally achieved [9])

HBAR-based sensors exploit two principal features yielding notable differences with other sensing solutions. The first one is related to the anisotropy of piezoelectric crystals on which these devices are built, which allows one for selecting crystal cut angles to optimize their physical characteristics. It is subsequently possible to choose cut angles to favor or minimize the parametric sensitivities of the considered wave propagation. The second remarkable feature of these devices concerns the use of piezoelectric excitation/detection of acousto-electric waves which allows for wireless interrogation in radio-frequency ranges such as ISM bands centered at 434MHz, 868MHz, 915MHz or even 2.45GHz.

This chapter presents HBAR principles and related applications. Specific acoustic and electrical behaviors of HBAR are discussed and the different ways devoted to the manufacture of these devices also are presented. Applications of HBAR such as oscillator stabilization, intrinsically temperature-compensated devices and sensors are finally reported. Further developments required to promote the industrial exploitation of HBAR are discussed to conclude this article.

2. HBAR principles

HBARs are constituted by a thin piezoelectric transducer above a high-quality acoustic substrate, as shown in figure 1. The piezoelectric transducer generates acoustic waves in the whole material stack along its effective electromechanical strength. Stationary waves are established between top and bottom free surfaces according to normal stress-free boundary conditions. As no electrical boundary condition arises at this surface, all the possible harmonics of the fundamental mode can exist. However, only the even modes of the transducer are excited as the only ones meeting the electrical boundary conditions applied to the transducer.

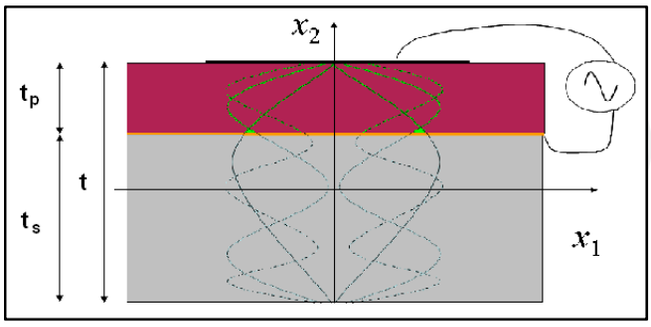

Figure 1. Schematic of HBAR

The electrical response of a HBAR can thus be interpreted as the modulation of the transducer resonance by the whole-stack bulk modes, presenting a dense spectrum of discrete modes localized around the resonance frequencies of the only piezoelectric transducer, as shown in figure 2. Since the substrate thickness is much larger than that of the piezoelectric film, most energy is stored in the substrate, and thus, the quality (*Q*) factor is

dominated by the acoustic property of the substrate. When the thickness of the substrate decreases, the device tends to behave as a FBAR (corresponding to t_s=0 in fig.1). Depending on both the material and the cut orientations of piezoelectric transducer, pure longitudinal or pure shear waves or combinations of these basic polarizations can be excited.

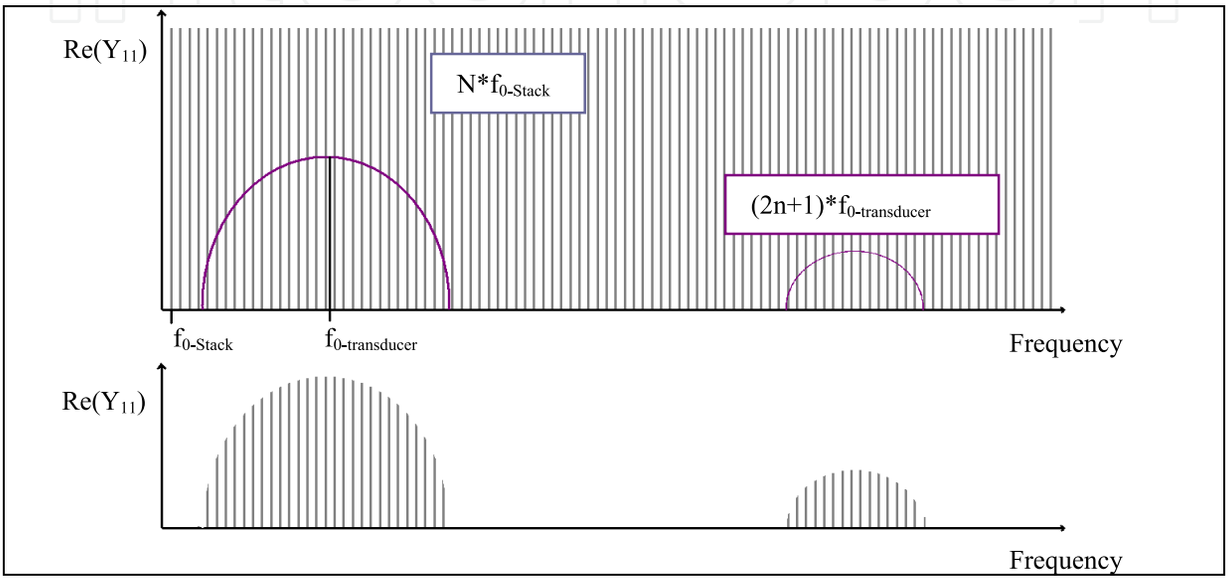

Figure 2. Schematic representation of the typical electrical response of HBARs.

Single port resonator structures can be easily achieved using HBARs, the use of two series devices being generally adopted to avoid etching the piezoelectric layer to reach the back electrode. Despite this favorable aspect, the exclusive use of single-port resonators limits HBAR applicability fields. Therefore, the possibility to fabricate four-port devices has been considered and experimentally tested (as shown in section 3.2). The leading idea consisted in transversely (or laterally) coupling acoustic waves between two adjacent resonators. The principle of such devices was inspired from the so-called monolithic filters based on coupled bulk waves in single crystals [10]. This is achieved by setting two resonators very close to one another. The gap between these resonators must be narrow enough to allow for the evanescent waves between the resonator electrodes to overlap and hence to yield mode coupling conditions. This system exhibits two eigenmodes with slightly different eigen-frequencies: a symmetric mode in which the coupled resonators vibrate in phase and an anti-symmetric mode in which they vibrate in phase opposition, as shown in figure 3. The gap between the two electrodes controls the spectral distance between the two coupled modes.

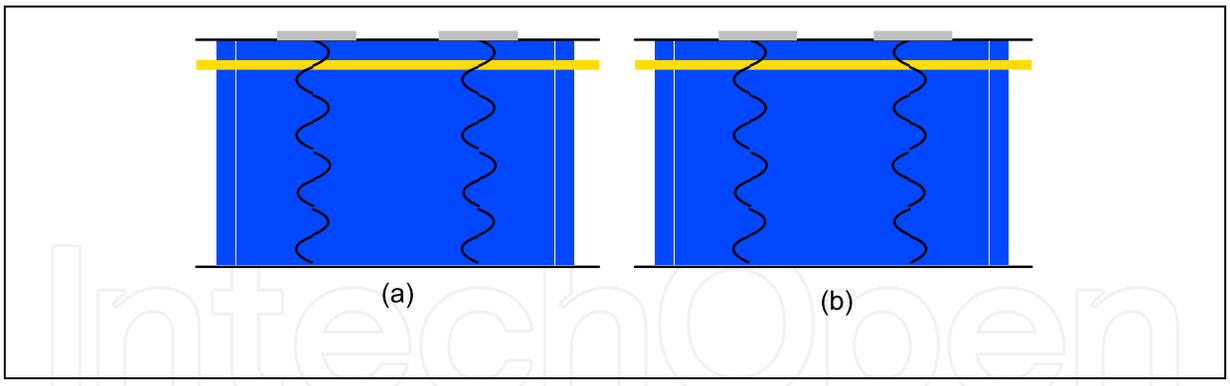

Figure 3. Principle scheme of the laterally-coupled-mode HBAR filter (a) symmetrical mode (b) anti-symmetrical mode

3. HBAR devices

3.1. Electrical and acoustic behavior

3.1.1. Single-port resonator

As explained above, the electrical response spectrum of such HBAR presents a large number of overtones. A large band representation allows for the observation of several envelopes themselves composed of several overtones. The central frequencies of these envelopes correspond to fundamental and even overtone resonances of the only transducer and therefore are mainly controlled by the transducer thickness.

Figure 4 shows the S_{11} response for the considered structure for different substrate thicknesses, illustrating the impact of this parameter on the overtone characteristics. The highest electromechanically-coupled overtone corresponds to the mode matching at best maximum energy location within the transducer, whereas the other overtones do exhibit smaller coupling factor proportionally to their spectral distance with the central overtone. The case of FBAR (t_s=0 μm in figure 1) is reported on this graph to effectively localize the central frequency of resonance and anti-resonance of the only transducer. In presence of a substrate, mode coupling between the two layers is made possible and several overtones appear for substrate thickness larger than the transducer one, as illustrated in figure 4. As suggested previously, the spectral distance between two overtones is mainly due to the substrate properties (velocity and thickness) when the later exhibits a thickness much larger than the other layers of the whole stack. Figure 4 also shows the evolution of the electromechanical coupling coefficient (generally noted k_s^2 for radio-frequency acousto-electric devices) when increasing the substrate thickness. The reduction of k_s^2 when increasing the substrate thickness is directly related to the energy ratio within the transducer and in the whole HBAR stack. Increasing the substrate thickness yields more energy in the whole HBAR structure and less energy within the transducer. Another interpretation consists in considering that the coupling of the transducer alone is spread on all the modes of the structure near the transducer resonance. Increasing the number of modes yields a reduction of the electromechanical of each mode coupled to the transducer mode. A trade-

off between the mode density and the stack thickness therefore is mandatory to optimize the HBAR response. Increasing the number of modes experimentally tends to provide higher quality coefficients for modes close to the transducer one but also reduces the corresponding coupling and significantly impact the device spectral density, yielding more difficulty to exploit well defined resonance.

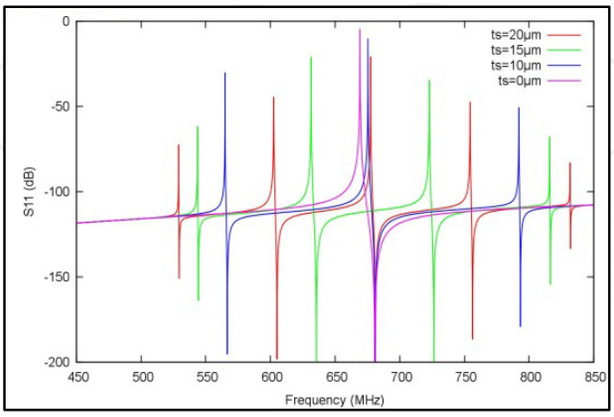

Figure 4. Impact of acoustic substrate. The reflection parameter-S11 with respect to a 50Ω load is measured for different substrate thicknesses. A material stack consisting of an acoustic substrate of $LiNbO_3$ (YX*l*)/163°, an aluminum electrode of 10nm thick, a 10µm thin piezoelectric layer of $LiNbO_3$ (YX*l*)/163° and a 10nm thick bottom aluminum electrode is considered here for a theoretical description of the HBAR characteristics. Electrode thickness are chosen extremely thin to neglect their acoustic influence. Acoustic and dielectric losses are only consider in $LiNbO_3$ layers for scaling the maximum achievable quality factors. For all computations, an active electrode surface of 100x100µm² has been considered for normative purposes.

For a given stack, the coupling coefficient of each group of overtones (these groups being defined by fundamental and even overtones of the transducer alone) depends on the material coupling coefficient of the transducer and on the order of the considered group. Indeed, the third order group presents a coupling coefficient divided by 9 compared to the fundamental group (one third of the fundamental mode coupling at excitation times one third at detection), the fifth is divided by 25, and so on. $LiNbO_3$ presents material coupling coefficient noticeably higher (3 to 7 times larger) than other material generally used for HBAR fabrication, such as AlN, ZnO. As a consequence, even transducer overtone groups can be effectively used with such a material and more especially when exciting pure shear waves as exposed further. Figure 5 shows the electrical response of a single-port HBAR built with (YX*l*)/163° $LiNbO_3$ piezoelectric layer and substrate. Only shear waves are excited and all even group can be visible from the fundamental to the 11th harmonic of the layer alone near 2GHz.

Each overtone in a given group presents a specific coupling coefficient k_s^2 and a specific quality factor Q. Central overtones present the highest coupling coefficients within a group, but not always the highest quality factors. Indeed, the substrate (Sapphire for instance) is usually chosen with acoustic quality better than the transducer material (Aln, ZnO) as it is expected to act as the effective resonant cavity, whereas the transducer material is selected for its piezoelectric strength. As explained above, the energy ratio within the transducer and

the substrate is higher for the central overtones than for the overtones located at the edge of the group.

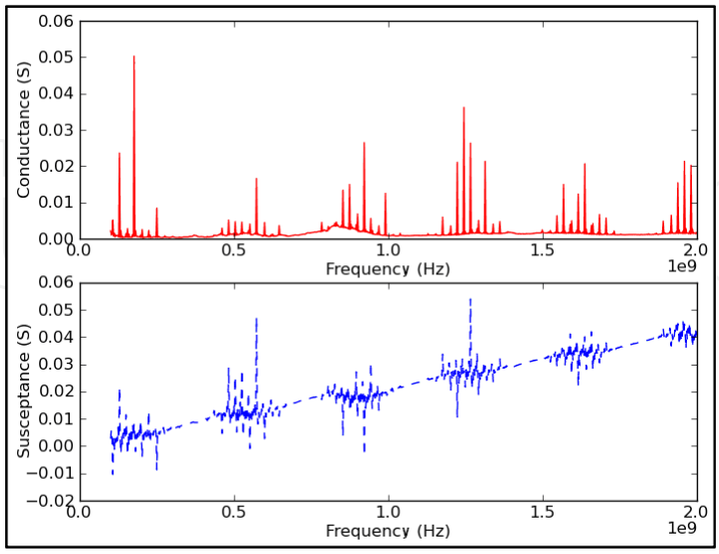

Figure 5. Single-port HBAR device built using $LiNbO_3/LiNbO_3$ (YX*l*)/163° cut.

In figure 6, a HBAR is constructed with $LiNbO_3$ material for the transducer. As shown further, $LiNbO_3$ presents better acoustic quality than Quartz, which is used for the HBAR substrate here to improve the device temperature stability (see section 4.2). In that example the overtone at 433.3MHz exhibits the best coupling coefficient k_s^2 as well as the best quality factor Q, due to the acoustic quality of $LiNbO_3$ compared to Quartz (see section 4.1).

According the above assumptions concerning material quality selection, the quality factor of overtones located at the edge of group is generally higher than the ones in the center of the group. Practically, it turns out that small-coupling overtones always exhibit better Q than the central overtones in a given group. One explanation of this objective result can be related to electrically generated losses (losses related to electrode resistivity and series resistance tends to increase with current).

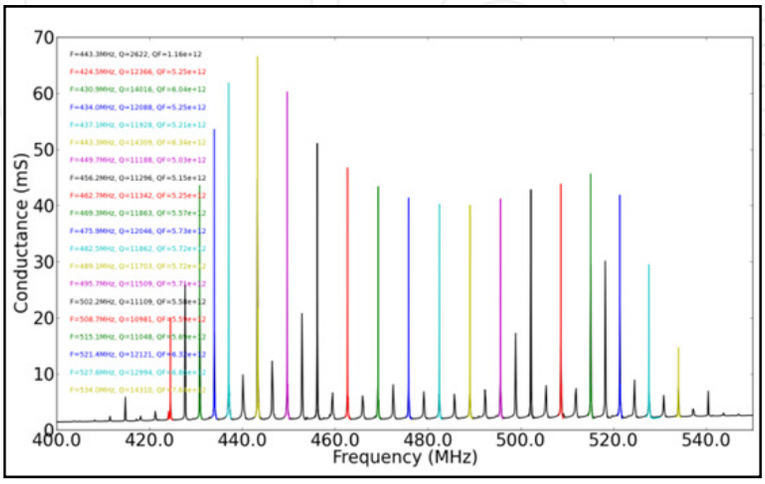

Figure 6. 5th Envelope of single-port HBAR device constituted by $LiNbO_3$ (YX*l*)/163°/Quartz.

3.1.2. Transversely-coupled HBAR

As explained above, the possibility to fabricate four-port devices has been considered and experimentally tested. Two HBAR resonators were fabricated on a $LiNbO_3$ (34µm) / Au (300nm) / $LiNbO_3$ (350µm) stack. Two 145x200µm² surface aluminum electrodes, were patterned upon the stack and separated by a gap of 10µm. Figure 7 shows a typical coupled-mode filter response for a device manufactured atop a $LiNbO_3$/$LiNbO_3$ structure. Rejection in excess of 20dB is demonstrated at 720MHz with a single filter cell. Insertion losses of about 15dB are emphasized and could be easily improved by impedance matching. The measured transfer function actually exhibits a double mode response, providing a first evidence of the device operation according to the above assumptions.

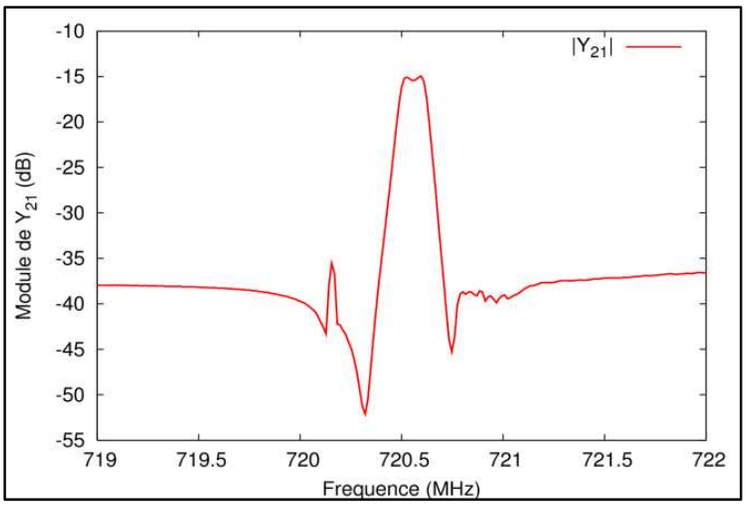

Figure 7. Four-port laterally coupled HBAR devices 0.1% band 720MHz $LiNbO_3$/$LiNbO_3$ filter.

Furthermore, the following experiment was applied for definitely validating the lateral mode coupling. The admittance of the first resonator was measured for two different loading conditions applied to the second resonator (Figure 8). For open circuit conditions, a main peak corresponding to the first resonator contribution is observed (Figure 8, left) together with a weaker contribution near the main resonance. For short-circuit conditions, the admittance measured on the first resonator shows two almost-balanced resonance peaks, (Figure 8, right). This behavior is explained by the fact that no current crosses the second resonator when in open condition, yielding a small contribution of the anti-symmetrical mode (due to poor boundary condition matching) whereas loaded electrical condition allows for an effective excitation of the later mode, yielding almost balanced contributions of symmetrical and anti-symmetrical modes as experimentally observed.

3.2. HBAR micro-fabrication

Two main approaches can be implemented to manufacture HBAR devices. The first approach consists in physical or chemical deposition of thin piezoelectric layers (such as ZnO, PZT, AlN and so on) onto the chosen substrate. The first HBAR was manufactured along this approach [11]. The main advantage of this kind of HBAR is the capability of the

related techniques (sputtering, epitaxy, sol-gel spinning/firing, pulsed laser ablation, *etc*.) to deposit thin layers which allow for achieving device naturally operating at high frequency (for instance in the vicinity of the 2.45GHz ISM Band, or even more). This approach also did provide among the highest *Q* factor ever measured for an acoustic-based resonator at room temperature [3], with *Q.f* product values in excess of 10^{14} at parallel resonance (7.10^{13} at series resonance).

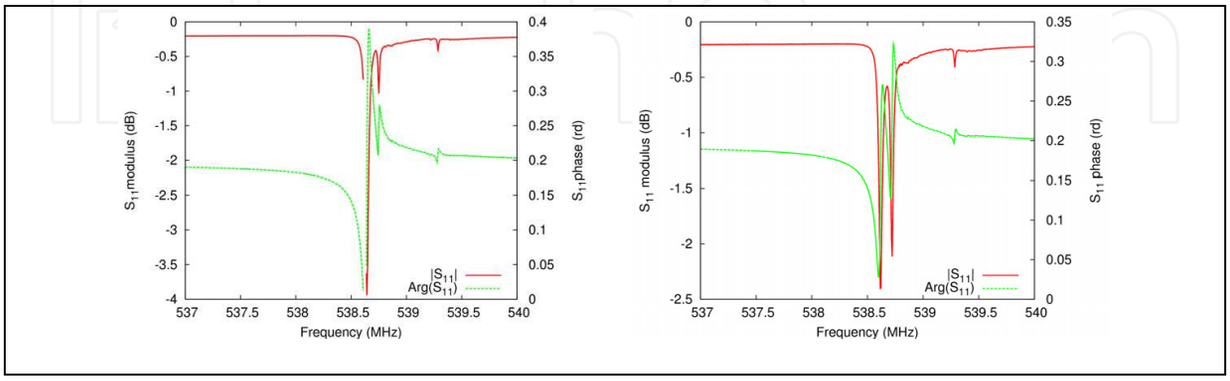

Figure 8. Admittances of one of the two resonators of the laterally-coupled structure as a function of the electrical conditions applied to the associated resonator (left) open circuit (right) 50Ω loading

Although this approach revealed efficient for operational device manufacturing, some drawbacks can be identified which limit the interest of the related resonators. Among these, one of the most problematic concerns the electromechanical coupling coefficient one can obtain particularly with AlN and ZnO, the most used thin piezoelectric layer for RF acoustic devices. As deposition techniques (principally reactive sputtering but also pulsed laser deposition (PLD)) generally allows for depositing well-controlled homogeneous C-oriented layers (i.e. with the C crystal axis oriented along the normal of the coated surface), the maximum accessible coupling remains much below 10%. Also the corresponding modes are purely longitudinal, with reduced degree-of-freedom for effectively controlled layer orientation suited for shear wave excitation/detection. Thin layers such as PZT can overcome this limitation but they generally exhibit notably high visco-elastic coefficients and significant dielectric loss which again limit their interest for high frequency (above 1GHz) applications. More generally, acoustic losses of most piezoelectric layers obtained by sputtering, sol-gel and techniques providing poly-crystalline materials always reveal larger than single-crystal ones. As explained before, the coupling coefficient of each high-overtone resonance depends on the number of overtones and on the intrinsic material electromechanical coupling coefficient. Poor material coupling coefficients prevent the use of overtones modulating the third (and therefore higher order) overtone of the piezoelectric transducer. Finally, compensating longitudinal modes thermal drift is particularly difficult as most of the high acoustic quality materials exhibit negative temperature coefficients of the corresponding phase velocity (as well as the transducer materials, ranging from -20 to -60ppm.K^{-1}). These negative aspects pushed to seek for other manufacturing approaches.

The opportunity to use single crystal layers for acoustic transduction therefore appears as an alternative solution. Assuming the possibility for manufacturing thin single-crystal films

atop any material stack makes possible the use of specific crystal cut to select the polarization of the excited acoustic waves as well as its electromechanical coupling coefficient.

The development of the so-called Silicon On Insulator (SOI(TM)) wafers has demonstrated the huge opportunities offered by the Smart Cut(TM) approach [12]. Moreover, its application for transferring single crystal Lithium Niobate thin layer into silicon proved to be effective for SAW device development [13]. As this technology requires a severe know-how and complex technological facilities and environment, an alternative fabrication technique based on metal diffusion at the interface between the materials to be bonded together [14] has been developed together with a lapping/polishing technique for HBAR manufacturing [15].

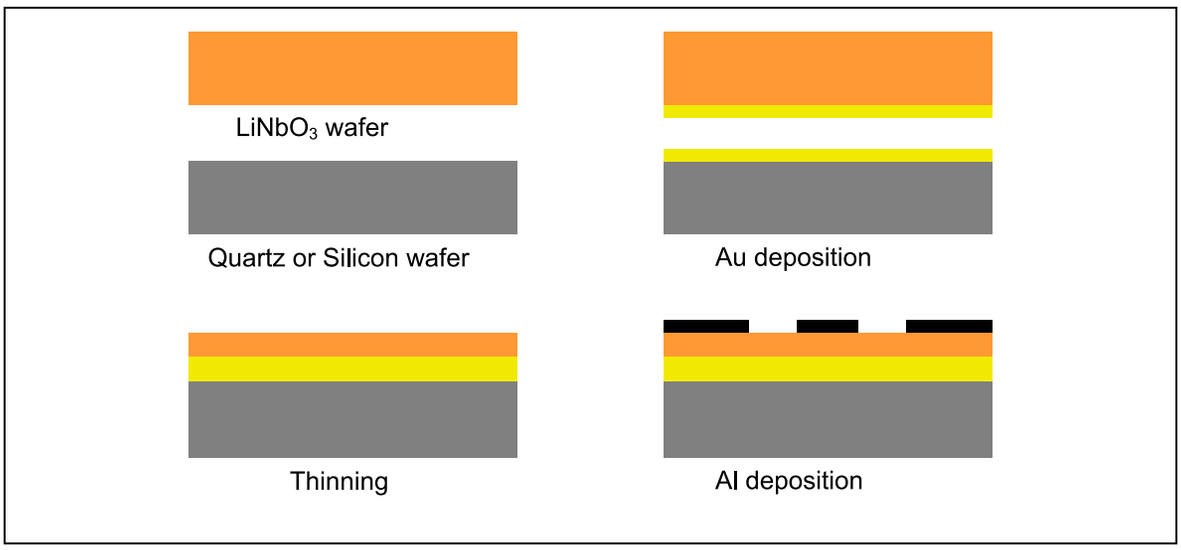

Figure 9. Process flow-chart for the fabrication of the HBAR based on bonding and lapping technology.

In this particular approach, contrary to the sputtering method, thermal process forbids to stack materials presenting notably differential thermal expansion coefficients. Smart Cut(TM) approach allows one to produce thin single crystal layers (such as $LiNbO_3$ for instance, or even $LiTaO_3$ [16]) with typical thickness below 1µm. Along this approach, embedded metal electrodes are fabricated using the Smart Cuttrade technology [16].

The above-mentioned bonding and lapping technology has specifically been developed to allow for material stacking at room temperature, for exploiting any material of any crystal orientation. The process flow-chart reported in figure 9 allows one for a collective manufacturing of HBAR devices. This process is based on the mechanical diffusion of sub-micron gold layers, providing an effective acoustic liaison of the chosen material as well as the HBAR back electrode at once. As the bonding operation is achieved at room temperature, no significant thermal differential effects are observed and the resulting wafer can be handled and further processed provided thermal budget remains smaller than 100°C (as experimentally observed).

Along the proposed approach, optical quality polished surfaces are preferred to favor the bonding of the wafers. A Chromium and Gold thin layer is first deposited by sputtering on

both wafers to bond ($LiNbO_3$ and Quartz in the example of figure 6 and 9). The $LiNbO_3$ wafer is then bonded onto the substrate by mechanical compression of the 200nm thick gold layers into an EVG wafer bonding machine as shown in figure 10. During the bonding process, the material stack is kept at a temperature of 30°C and a pressure of 65N.cm^{-2} is applied on the whole contact surface. The bonding can be particularly controlled by adjusting the process duration and various parameters such as the applied pressure, the process temperature, the quality of the vacuum during the process, *etc*. In the reported development, the process temperature is kept near a value close to the final thermal conditions seen by the device in operation. Since substrate and piezoelectric materials have different thermal expansion coefficients, one must account for differential thermo-elastic stresses when bonding both wafers and minimize them as much as possible.

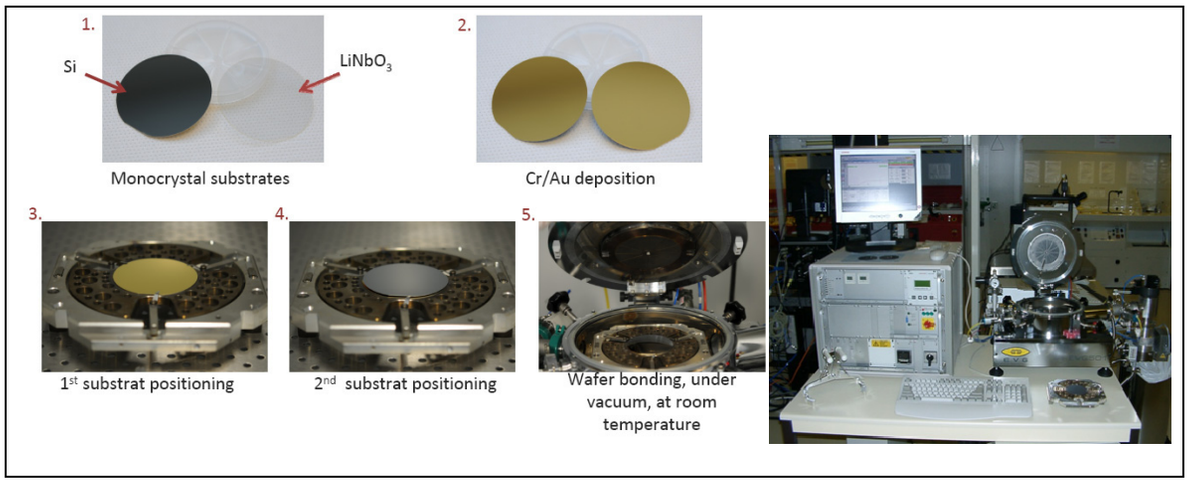

Figure 10. EVG wafer Bounder and illustration of Gold bonding process.

Once the bonding achieved, it is necessary to characterize the quality of the bonding. Due to the thickness of the wafers and the opacity of the stack (metal layers), optical measurements are poorly practicable. To avoid destructive controls of the material stack, ultrasonic techniques have been particularly considered here. The reliability of the bonding then is analyzed by ultrasonic transmission in a liquid environment. The bonded wafers are immersed in a water tank and the whole wafer stack surface is scanned. Figure 11 presents photography of the bench. Two focused transducers are used as acoustic emitter and receiver. They are manufactured by SONAXIS with a central frequency close to 50MHz, a 19mm active diameter and a 30mm focal length. The beam diameter at focal distance at -6dB is about 200µm.

Such a lateral resolution enables one to detect very small defects. The principle of the characterization method is based on the measurement of the received acoustic amplitude which depends on the variation of the acoustic impedance of the bonding area. If the bonding presents a defect at the interface between the two wafers, a dust or an air gap in most cases, the reflection coefficient of the incident wave is then nearly 1. The amplitude of the received wave is strongly reduced or even vanishes. Figure 12 shows a C-Scan of a Silicon/$LiNbO_3$ wafer bonding characterization. The blue color corresponds to bonded surfaces, whereas yellow and green regions indicate bonding defects.

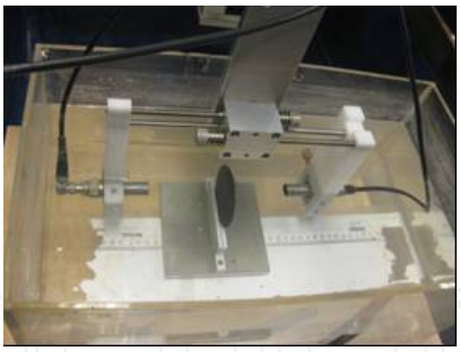

Figure 11. Ultrasonic characterization bench dedicated to non destructive control of the bonding interface.

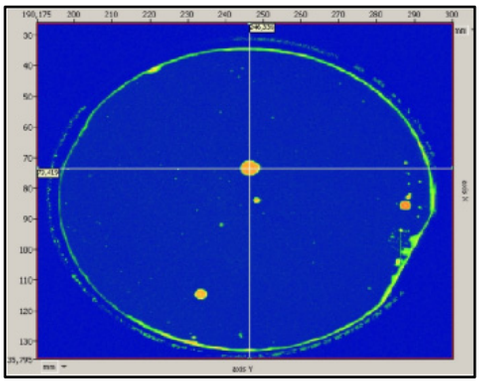

Figure 12. Characterization of a Silicon/LiNbO3 bonding – surfaces are bonded at 95%.

This method presents three major advantages:

- The control of the bonding can be made during the polishing steps without destruction; or the control can be done at the end of the process, indeed, the different layers obtained by sputtering do not disturb the measure.
- There is no constraint related to time resolution as in pulse-echo method, as the wafer thickness is not dramatically larger than the wavelength.
- The analysis of the ultrasonic transmitted signals is very simple because only the amplitude of the first detected signal contains the useful information.

Figure 13. SOMOS lapping/polishing machine.

The piezoelectric wafer is subsequently thinned by lapping step to an overall thickness of 20μm. The lapping machine used in that purpose and shown in figure 13 is a SOMOS double side lapping/polishing machine based on a planetary motion of the wafers (up to 4" diameter) to promote abrasion homogeneity. An abrasive solution of silicon carbide is used here. The speed of the lapping is controlled by choosing the speed of rotation of the lapping machine stages, the load on the wafer, the rate of flow or the concentration of the abrasive. Once close to the expected thickness, the lapping process is followed by a micro-polishing step. This step uses similar equipments dedicated to polishing operation and hence using abrasive solution (colloidal silica) with smaller grain. This polishing step is applied until the average surface roughness r_a remains larger than 3nm. Afterward, the wafer is considered ready for surface processing.

The final step of the HBAR fabrication is the deposition and patterning of the top-side electrode. Aluminum electrodes are then deposited on the thinned $LiNbO_3$ plate surface with a lift-off process. This top electrode allows for connecting the HBAR-based sensor and for characterization operations.

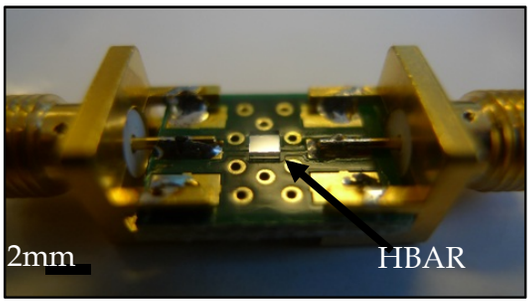

Figure 14. Flip chip of HBAR resonator on PCB substrate.

For all HBAR device, one technological problematic concerns packaging. Due to the HBAR operation, both sides must be kept free of any stress or absorbing condition. HBAR packaging therefore requires specific developments to meet such conditions. Experimental developments reveal that flip-chip techniques are the most appropriate approach in that purpose (as shown in figure 14).

4. HBAR optimization

4.1. Minimizing losses in HBARs

Since the 80's, HBAR devices have demonstrated high quality factor at high frequencies compared to other acoustic devices such as BAW, SAW. *Q.f* products around 1.1×10^{14} have already been obtained for high overtones using aluminum nitride (AlN) thin films deposited onto sapphire [3]. Hongyu Yu *and al.* showed HBAR with a structure of 0.10μm Al /0.88μm ZnO /0.10μm Al /400μm Sapphire which was measured to have a loaded *Q* of respectively 15,000 and 19,000 for series and parallel resonant frequencies around 3.7GHz. The temperature coefficient of the resonant frequency is -28.5ppm/°C [17]. Resonators obtained by $LiNbO_3$ wafer as a transducer bonded on another $LiNbO_3$ wafer used as the HBAR

substrate exhibit *Q* factors of 53,000 at 1.5GHz using the Gold bonding technique [5] and *Q.f* product above 8.10^{13} with an 800nm thickness for the piezoelectric layer by Smart Cut approach [18]. Understanding losses phenomena helps to design high quality factor devices. Loss origins can be classified into two categories: material (intrinsic) and geometry (technology-related). Due to the architecture of HBAR, the quality factor of such devices depends on the crystalline losses and on the material isotropy, on the surfaces parallelism and any loading due to the electrodes.

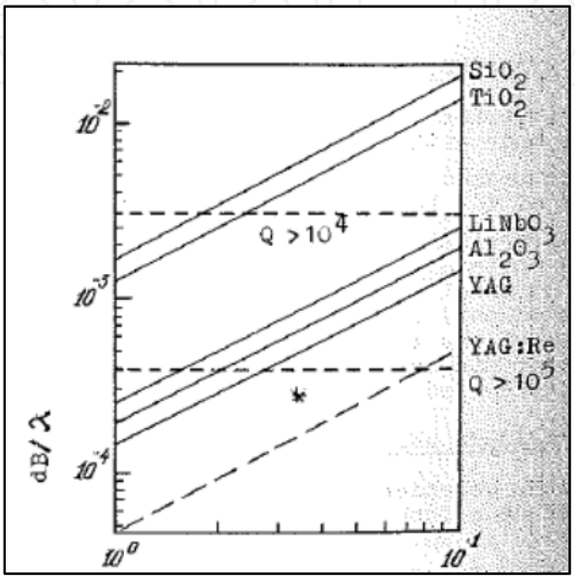

Figure 15. Losses per wave length and the resonator's quality *Q* as a function of frequency (GHz) for various materials [19].

As explained before, the quality factor is directly link to the acoustic quality of the substrate. Some works have already been done to compare and improve materials to favor high acoustic resonance quality [19], [11]. Figure 15 shows an example of these works [19].

The polishing process providing damaged-free ultra-smooth surfaces is essential, as well as checking the substrate quality by X-ray topography. To take into account current industrial needs, using the technology of material crystal growth is crucial to obtain large wafers. In this context, $LiNbO_3$, $LiTaO_3$ Sapphire, and YAG are the preferred candidates as they do present effective acoustic quality (*i.e.* reduced visco-elastic and dielectric damping properties) and available as 4 inch wafers, excepted for YAG substrates.

The defect of parallelism between two surfaces of HBAR devices dramatically limits the quality factor [11]. Figure 16 shows the quality factor of HBAR modes on Sapphire-base structures versus the plate tilt. As clearly highlighted by this graph, the parallelism must be perfect to prevent power flow yielding *Q* factor limitations. For example, a HBAR built on a 4 inch wafer with a total thickness variation (TTV) of 3µm (commercially accessible for Silicon) does not suffer from any parallelism defect and therefore the quality of its resonances is almost not limited by this effect ($Q>10^5$). However, one can see that a thickness variation of 3µm on 1cm yields effective limitation of the quality factor ($Q<10^4$).

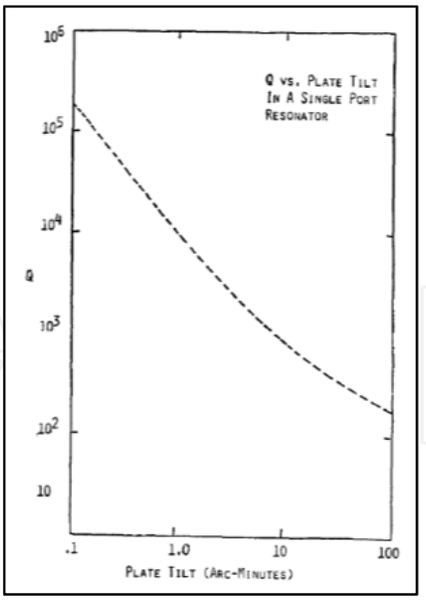

Figure 16. Parallelism-limited *Q* in a single-port resonator built on Z cut Sapphire substrates [11].

The shape, size and nature of the electrodes can be also important to manufacture high *Q* HBAR devices. Some works have been done on electrodes of HBAR devices [20], [21], [22], [23].

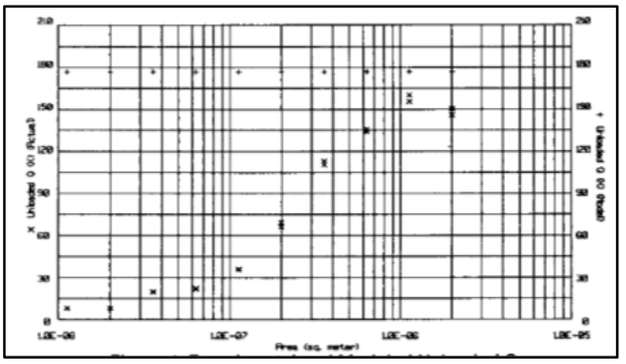

Figure 17. Experimental and Modeled Unloaded Q versus aperture [20].

D. S. Bailey *and al.* showed that the HBAR does not follow the one dimensional computer model [20]. Indeed, figure 17 shows the difference between the experimental *Q* and the theoretical *Q* versus the aperture of the electrode. The difference is due to the diffraction effect. The optimum electrode area can depend on two main parameters: the clamp capacitance C_0 and the geometry. This capacitance C_0 is proportional to the surface area and influences other parameters of resonator such as difference in impedance at series and resonance frequency. With a large active area, defects in transducer crystal or of geometry can happen more easily. The optimization of the area shape and surface to limit the diffraction effect and improve the quality factor is an area of ongoing works.

Furthermore, for ultra-high frequency HBAR devices, the electrodes are not thin compared to transducer layer. The thickness and the nature of electrodes have an influence on the quality factor and the other parameters such as the electromechanical coupling coefficient and the resonance frequency. Many works have been done on this subject [23], [24], [21].

The conditions of metal sputtering can influence the nature of the metallic electrode. Indeed, the conditions of metal sputtering for thin layers modify the density and the rate of impurity of the layer. The optimum must be found to have the highest metal density with the lowest impurities. Furthermore, some works compare the influence of different metallic layers (Al, Au, W, Ag) on the quality factor. If we consider the modified Butterworth-Van Dyke (MBVD) model, the best electrode is constituted with the lowest resistivity (Au), but experimentations also show the influence of other parameters. Thus, a Molybdenum layer used as an electrode shows better results due to better acoustic impedance [23].

Generally speaking, low losses applications also require a temperature compensation for the resonator. One solution is to have intrinsic compensation of temperature and it is the purpose of the next paragraph. Another solution is to control frequency by measuring temperature.

4.2. Temperature compensation

One challenge of the radio-frequency bulk acoustic devices is the temperature stability of their resonance frequency. A lot of work has been achieved exploiting thin piezoelectric films for developing temperature-compensated HBARs, with various successes. The possibility to use single crystal thinned films appears as an alternative to control the piezoelectric film properties (velocity, coupling, temperature sensitivity, and so on.) and to globally reconsider material association according to the technological assembly process previously presented.

The celebrated Campbell&Jones method [25] is used here for predicting the Temperature Coefficient of Frequency (TCF) of any mode of a given HBAR. As it has been reported hundred times in previous papers, only the main basic equation is reported below:

$$f = \frac{v}{2e} \rightarrow \frac{df}{f}(T) = \frac{dv}{v}(T) - \frac{de}{e}(T) \tag{1}$$

f, e, v and T are respectively frequency, thickness of resonator, wave velocity and temperature.

Which means that the frequency changes due to temperature variations is computed as the difference between the development of the velocity and of the stack thickness versus temperature. Theoretically using a standard anisotropic 1D model reveals that zero temperature coefficients of frequency (TCF) can be obtained and optimized along the mode order. It is well-known that Quartz and fused Silica (glass) do exhibit positive TCFs. So the use of the other temperature-compensated Quartz orientations, and hence of any other material sharing such property, has been checked theoretically and reveals applicable as well.

As example, Lithium of Niobate and Quartz have been associated for the fabrication of shear-wave based HBARs. $LiNbO_3$ provides crystal orientations for which very strongly coupled shear waves exist (k_s^2 in excess of 45%) whereas AT cut of Quartz allows for

compensating second order frequency-temperature effects [WO2009156658 (A1)]. Although this idea was already proposed using other material combinations [US Patent #3401275A], no real design process was presented until now and therefore the possibility to actually determine structures allowing for high frequency operation with first order TCF smaller than 1ppm.K^{-1} was quite hypothetical, but improvement of numerical tools allows this design.

Nevertheless, some works show the possibility to have an intrinsic compensation of the temperature for HBAR devices [8], [26]. Figure 18 shows the temperature dependence for different configuration of HBAR devices constituted by $LiNbO_3$ and Quartz layers with different cut orientations. This work shows clearly that the choice of materials and the cut orientation of these materials have a direct impact on the frequency shift with temperature variations [26].

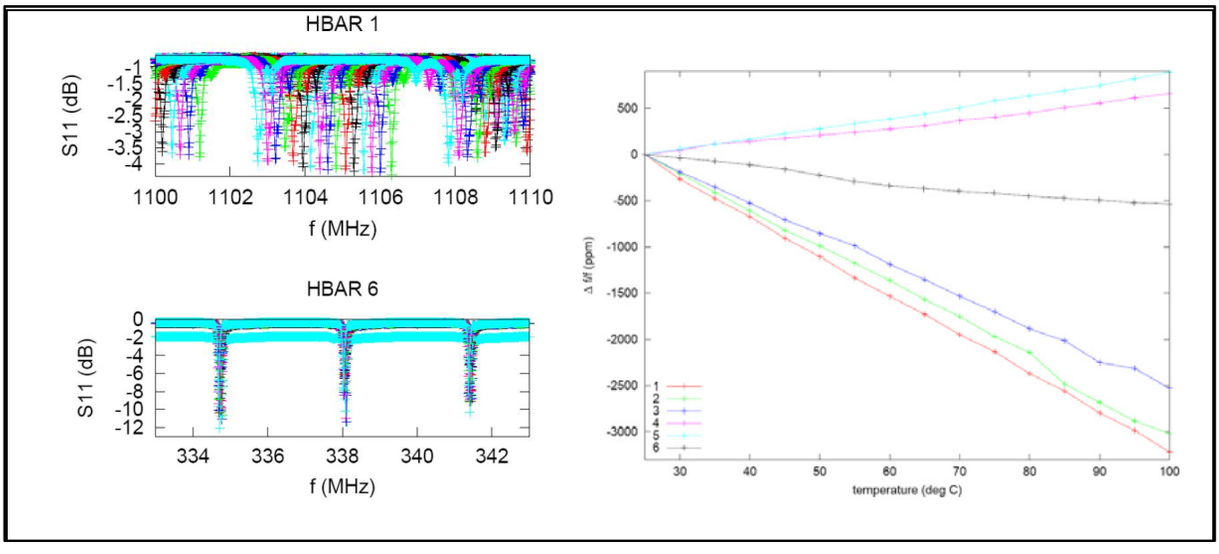

Figure 18. Electrical responses for two different configurations of HBAR (left), frequency variation versus temperature for six configurations of HBAR (right) [26].

Moreover, the frequency dependence on temperature is different for each overtone of HBAR devices. The thickness ratio between the transducer layer and the substrate also influences the frequency variations with different temperatures. Figure 19 shows the computation of the temperature coefficient of frequency (TCF) of a HBAR for various Lithium of Niobate / Quartz thickness ratios. This HBAR device is built on a (YX*l*)/163° $LiNbO_3$ thinned plate bonded on (YX*lt*)/36°/90° Quartz substrate of 50µm [27]. One can see that depending on the harmonic number, the TCF_1 changes from +1 to -14ppm.K^{-1}. Furthermore, depending on the harmonic of the transducer alone, the TCF_1 may notably change and thus it cannot be considered as a simple periodic function versus harmonic number. Therefore, it is mandatory to accurately consider all the actual features of the structure for an accurate design of a resonator, *i.e.* the operation frequency, the harmonic number and the thickness ratio for a given structure. To complete this, one should also account for the actual thickness of the device as this parameter will control the possibility to select one (frequency/harmonic number) couple. Finally, it clearly appears that the analysis of such HBAR TCF requires a

numerical analysis and that if an intuitive approach allows for a first order definition of crystal orientations, the complicated distribution of energy within the stack versus all the structure parameters induces more intrication in the design process.

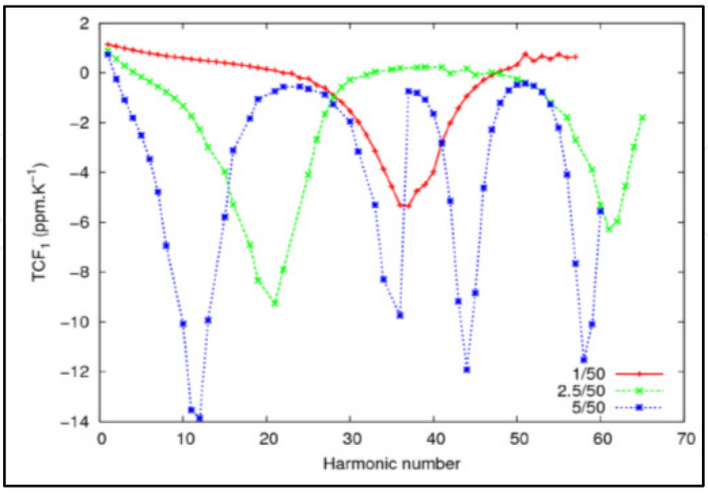

Figure 19. Plot of TCF of a HBAR built on a (YX*l*)/163° LiNbO3 thinned plate bonded on (YX*lt*)/36°/90° Quartz substrate for various Lithium of Niobate/Quartz thickness ratio (Quartz thickness arbitrary fixed to 50 μm) [27].

5. HBAR applications

5.1. HBAR sensors

Industrial acoustic-resonator-based sensors require adapted electronics to be efficiently operated. Two main approaches have been developed in that purpose:

- The first way is to use the acoustic resonator in an oscillator loop. Compared to normal oscillator use in frequency/time applications, some specific operation regimes must be considered for sensors [28]. Particularly, the resonance frequency is assumed to drift along the measured parameter on a large frequency domain. The *Q*-value of the resonator may notably vary as well as other parameters like electromechanical coupling and the overall electrical conductance (connected one another) yielding the need for improved electrical robustness of the circuit. The electronics therefore must be able to adapt its operation parameters. Distance between electronic and sensor is often important compare to classic oscillator. Due to these reasons, resolution of the system is limiting to 1.10^{-8}. As example, sensors at 434MHz have resolution limitation of 5Hz due to oscillator loop measurement method. Finally, to use this method, we need resonator with low harmonic generation. BAW, SAW and FBAR can use this electronic.
- The second way is to have electronic interrogation which finds frequency resonance in determined range of frequency. With classic method it is possible to obtain 100Hz of resolution for 434MHz sensors [28]. If electronics is improving, we can achieve 5Hz of resolution for 434MHz sensors [29]. In this case, clock of electronic is really important for performance. All kind of resonators sensors can be interrogated by this technique, especially HBAR device which present high overtone generation.

Acoustic sensor is passive sensor. Device combine with antenna could be having great interest. Indeed, electromagnetic waves can be changed on electrical waves on electrodes, which can excite acoustic waves by piezoelectric effect. Furthermore this phenomenon is linear and invertible. So, wireless interrogation is possible with acoustic sensors. Wireless communication presents great interest for all hard environments. In that way, acoustic sensors can be use in engine, close environment and more generally in all environments where wire can not be employed.

With wireless interrogation, antenna size, quality factor of resonator, frequency have a strong impact. With increasing of frequency, antenna size decrease. Indeed, the size of antenna is equal to the quarter of wavelength. When higher ISM band is used, quality factor need to be increase to give the same obstruction of the ISM bandwidth. At -3dB, the bandwidth of resonator is proportional to frequency divided by quality factor. And finally, the flight time is proportional to quality factor divided by frequency. They are two consequences of this flight time. Firstly, to have enough energy when frequency increase, the quality factor need to increase. As example, SAW resonators at 434MHz ISM band have quality factor of 10,000 and can be interrogated by wireless approach. To pass at 2.45GHz ISM band, a quality factor equal to 20,000 is required. HBAR devices achieve these characteristics. Secondly, refresh rate increases with frequency. With bandwidth of few kHz the refresh rate is around one millisecond. In this case, quality factor of sensor could not be too higher. So, quality factor of HBAR device need to be optimize for wireless sensor application.

HBAR devices present a great advantage for achieving sensors device. As previously discussed, frequency shift due to temperature effects can be minimized and even compensated, but also magnified as well. As a consequence, HBAR temperature sensors are considered first. Moreover, due to high number of overtones of such devices, it is also possible to develop sensors exhibiting different sensitivity to a given parametric effect at different frequencies. Acoustic devices can also be effectively exploited as stress sensor or pressure sensors. The fabrication of SAW pressure sensor based on thinned Quartz membrane (for instance) was strongly investigated due to the dependence of the wave velocity versus tensile stress at the surface of the membrane when bent by pressure. In the case of bulk wave propagating in such a membrane, the strain variations across the membrane thickness forbid the use of such an approach to develop pressure sensor applications. This can be easily demonstrated using for instance static finite element analysis with a very simple mesh. Indeed, the strain and hence the stress change their signs along the membrane thickness when submitted to pressure. As a consequence, the strain variation across the HBAR generates equilibration of the velocity variations. On the one hand, the strain below the membrane neutral line yields an increase of resonant frequency of the HBAR; on the other hand, the strain above the neutral line yields a decrease of this frequency. Consequently, the resulting frequency shift is negligible. One solution consists in the fabrication of a micro-cavity within the HBAR stack near the neutral line. If the transducer of the HBAR structure is straight above this micro-cavity, the emitted bulk waves are reflected by this micro-cavity and hence confined in this membrane location. The

micro-cavity then plays the role of a mirror for the waves. The structure of such device is shown in figure 20. The surface of the cavity should at minimum coincide strictly to the surface of the transducer, but to ease the fabrication (particularly to manage alignment issues) the cavity largely overlaps the transducer aperture. The micro-cavity/micro-mirror could be placed at different deph into the HBAR stack. Its location will define the HBAR sensibility to stress [8].

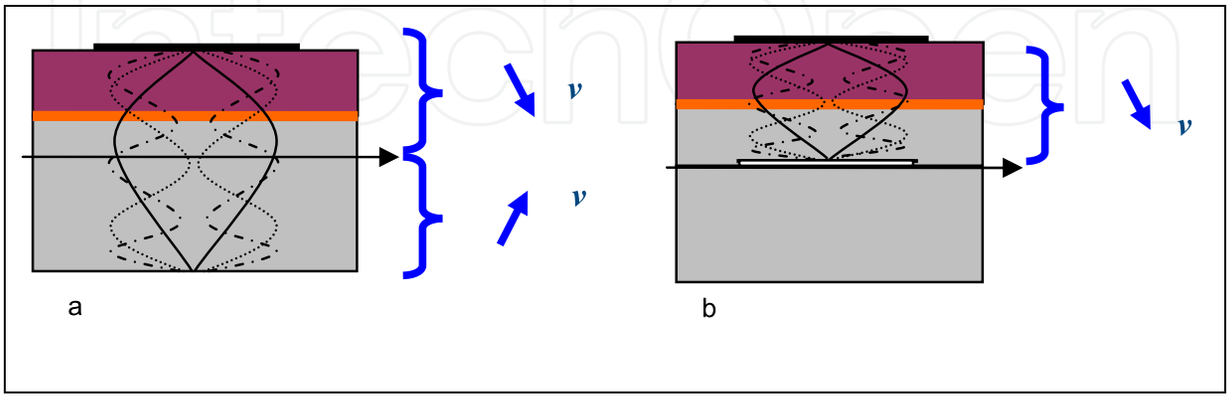

Figure 20. HBAR structures presented low frequency sensitive to stress (a), and highly frequency sensitive to stress with the realization of micro-mirror under the transducer aperture [8].

A lot of works has been done on liquid or gaz HBAR / FBAR sensor and as most representative example, gravimetric sensor. The basic principle of gravimetric acoustic wave sensors is the measurement of the phase velocity variations due to an adsorbed mass or a layer thickness change atop the device during a chemical reaction: this phase velocity is dependent on the boundary conditions of the propagating acoustic wave and is affected either by the layer properties or its thickness. The usual principle exploits bulk acoustic waves, yielding the well-known concept of Quartz Crystal Micro-balance (QCM). The gravimetric sensitivity of the QCM is directly related to its thickness and as a consequence to its fundamental frequency f_0. Adsorption on one side of the resonator modifies its resonance conditions and thus allows for a gravimetric detection. Furthermore, it is possible to functionalize the surface with specific reactants to provide information on the concentration of the adsorbed (target) species in the medium surrounding the sensor [31]. The case of HBAR is particularly attractive as one can expect probing the adsorbed material at various frequencies, providing frequency-dependent information such as viscosity for instance.

Copper electro-deposition on the back side of a HBAR has been used for calibrating the gravimetric sensitivity of its overtones. This approach was particularly implemented as it provides an independent estimate of the deposited metal mass through the measurement of the current. A negative current indicates copper reduction (deposition on the working electrode) whereas a positive current indicates oxidation (copper removal from the working electrode). Simultaneous to the current monitoring, the acoustic phase and magnitude at fixed frequency are recorded [30]. The figure 21.a shows four different overtone frequencies (red dot) recorded. Figure 21.b. shows relative frequency variations and clearly shows the sensitivity difference of the four HBAR overtones. Sensitivity of gravimetric HBAR directly

depends on the stack thickness and more precisely on copper thickness versus transducer thickness. The best gravimetric HBAR sensor is constituted by the thinnest stack with metallic thickness equal to quarter of wavelength [31].

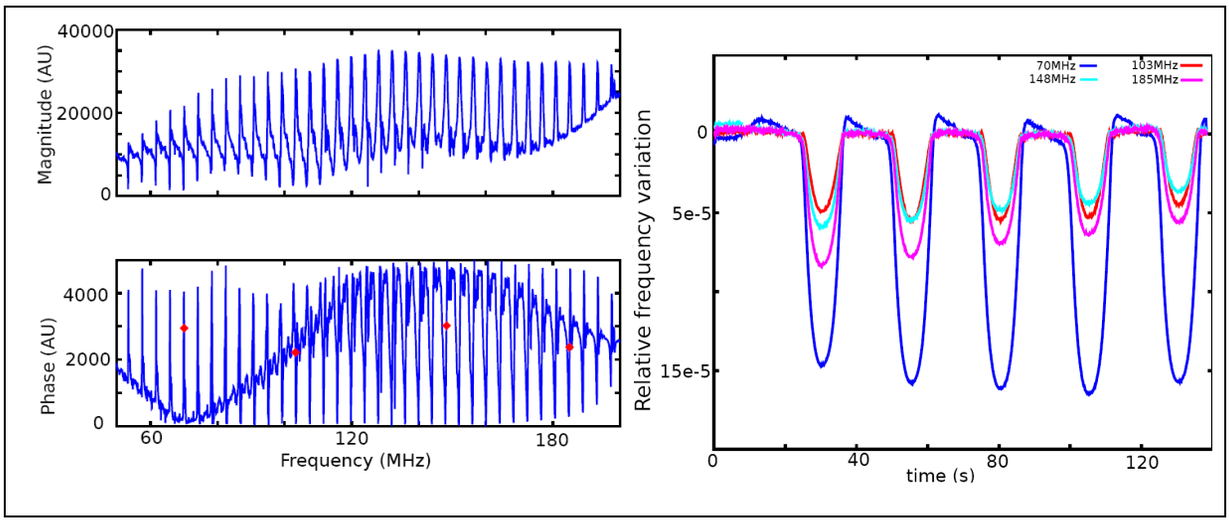

Figure 21. (a) Overtones of the fundamental transducer layer mode of a gravimetric HBAR sensor with four probed frequencies (red dot), (b) relative frequency variations of these four frequencies with their relative sensitivities [30].

5.2. HBAR-stabilized oscillators

Radio-Frequency oscillators can be stabilized by various resonating devices. Their stability is mainly conditioned by the spectral quality of the resonator even if the oscillator loop electronics must be optimized to lower the generated noise as much as possible. For mid-term stability, temperature compensation is a key point and allows for notably improving the corresponding figures of merit. The possibility to build temperature compensated HBARs has been shown in paragraph 4.2 and is a key-point for the fabrication of oscillator exhibiting short-term stability compatible with practical applications.

Moreover, the frequency stability of an oscillator can be characterized by its single-sideband phase noise, $L\{f_m\}$. Leeson's equation [33] shows that low phase noise operation can be achieved by increasing the loaded quality factor Q_{load} of the resonator. According to Leeson's model, a high resonator quality factor (Q) or circulating power level improves the phase noise and, therefore, the short-term stability of the oscillator. Considering these aspects, HBAR device features for the frequency stability reveal more favourable than FBAR or SAW device ones. Therefore HBAR should allow for notably improving oscillator performances. However, multi-overtone features of HBAR do not facilitate resonance lock for oscillator applications. Therefore SAW or FBAR device are generally used to filter the frequency of HBAR. Consequently, the compactness of HBAR is deteriorated due to the need for this filter. Optimizing HBAR spectral response then is still an open question and should receive more attention in future developments. One can note that using single port HBARs with optimized frequency separation between the overtones [32] may allow to get rid of this filtering operation.

HBAR then are capable to address high frequency source applications without requiring multiplication stages as usually achieved. The idea then is to evaluate the effective interest of HBAR for direct frequency synthesis, reducing the oscillator architecture complexity and potentially improving the corresponding operational features.

Hongyu Yu and *al.* have presented a local oscillator based on a HBAR resonator associated to an atomic clock [34]. Atomic clocks are used for embedded applications which need high stability performance such as GPS station. The atomic transition allows having long-term stability in this application, but it presents poor short-term stability. To success oscillator based on this atomic transition, local oscillator is needed. This local oscillator stabilizes the short-term variation of the global oscillator with its short-term performance. The local oscillator need to have good phase noise (better than -70dBc/Hz at 1kHz for instance) to prevent global degradation of clock stability. Figure 22 shows the phase noise measurement data of the 3.67GHz Pierce oscillator and the 1.2GHz Colpitts oscillator, and the Allan deviation of the free-running 3.67GHz oscillator that consumes only about 3mW [34]. Local oscillator based on HBAR resonator need frequency control to achieve the atomic transition frequency. With the modulation of the HBAR frequency with an external synthesizer and FBAR filters, the local oscillator locked to the coherent population trapping resonance.

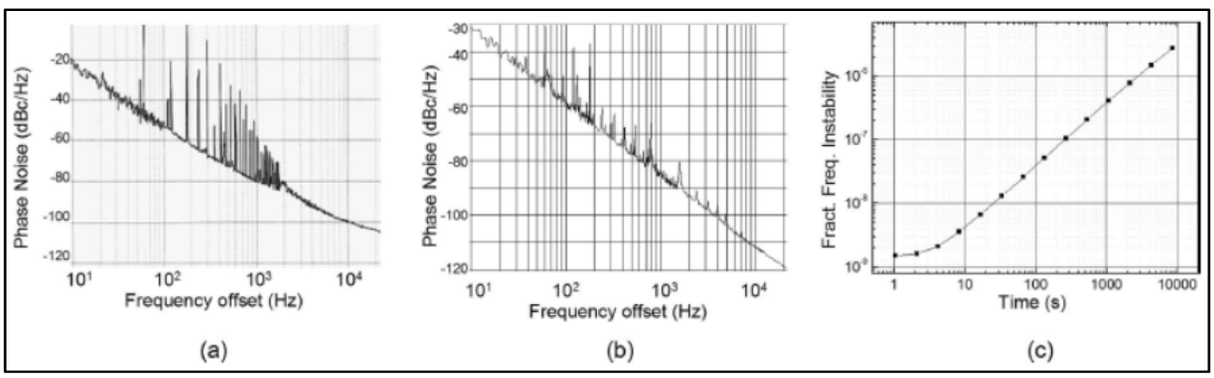

Figure 22. Phase noise measurement data of (a) the 3.67GHz Pierce oscillator and (b) the 1.2GHz Colpitts oscillator. (c) Allan deviation of the free-running 3.67GHz oscillator that consumes only about 3mW [34].

Other applications require low phase noise oscillator such as embedded RADAR. A radio-frequency oscillator operating near the 434MHz-centered ISM band validates the capability of the above-mentioned HBAR for such purposes. The composite substrates have been built using 3-inches (YX*l*)/163° $LiNbO_3$ cut wafer bonded and thinned down to 15µm onto a 350µm thick (YX*lt*)/34°/90° Quartz base. Single-port resonators operating near 434MHz (exploiting the third harmonic of the thinned Lithium of Niobate plate as the HBAR "motor") have been then manufactured. Electrical and thermoelectric characterizations have shown quality factor of the resonance in excess of 20,000, yielding a *Q.f* product of about 10^{13} and a third order frequency-temperature behavior. A SAW filter was used to select the ISM band and to filter the high spectral density HBAR response (figure 23). The oscillator then has been measured using a phase noise automatic bench. A phase noise better than --160dBc/Hz at 100kHz has been measured as well as a -165dBc/Hz level at 1MHz from the

career (figure 23). Short-term stability characterizations show that the resonator stability is better than 10^{-9} at room conditions (no temperature stabilization).

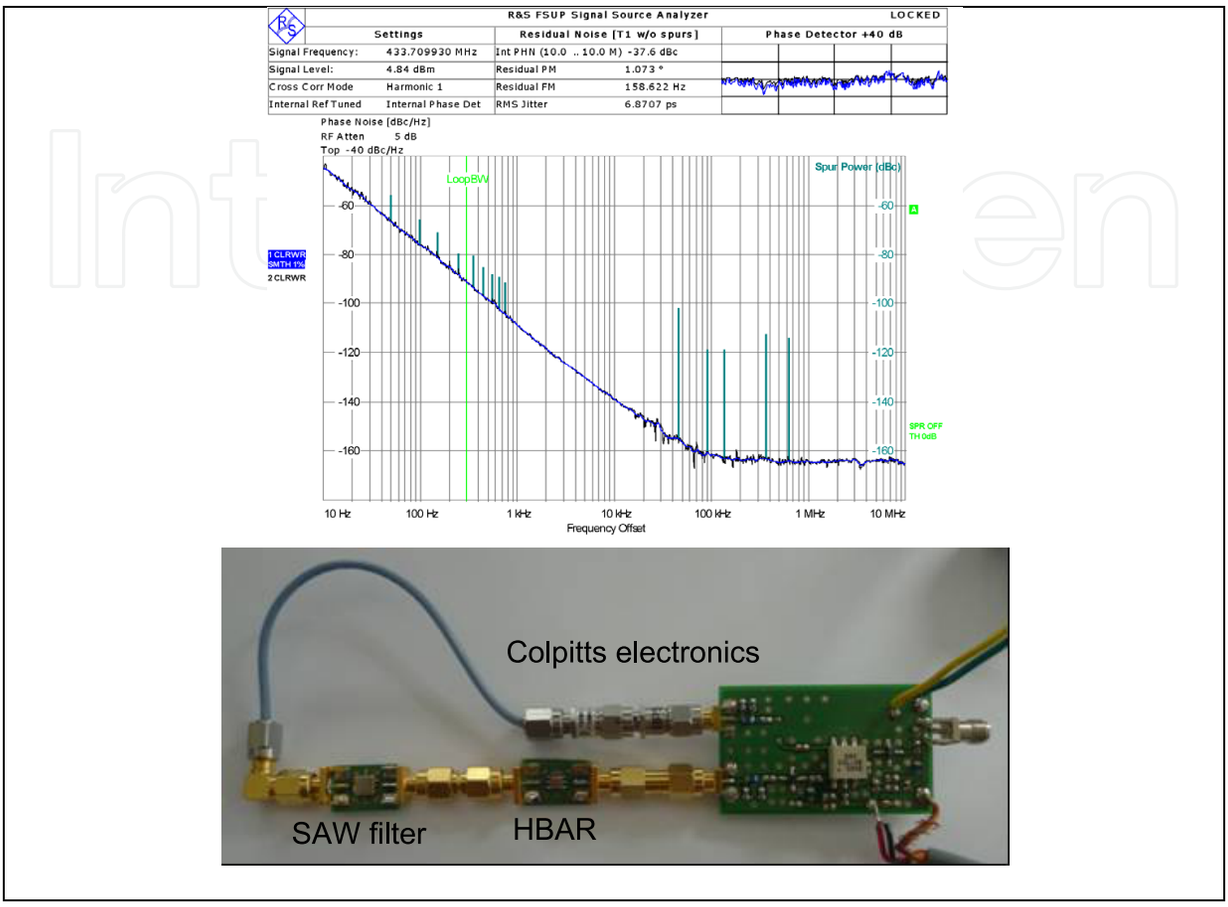

Figure 23. Phase noise curves for oscillators at 434MHz constituted by High Overtone Bulk Resonator, SAW filter and Colpitts electronics.

To achieve higher frequency (above 1GHz), four-port resonators are mandatory due to the difficulty to adjust the oscillator tuning elements. For this application, the temperature stability is required and therefore the resonator exploits a (YX*l*)/163° $LiNbO_3$ thinned layer atop a (YX*lt*)/36°/90° Quartz substrate. The electrodes defining the coupled transducers (four-port resonator) are two half-circles (300µm diameter) separated by a gap of 20µm, yielding favorable conditions for using the resonator to stabilize an oscillator loop at 935MHz and 1.636GHz. The device were cut and packaged, mounted in an oscillator loop, and measurements of phase noise were performed. Figure 24 shows the phase noise of the two corresponding oscillators compared with the phase noise of an oscillator stabilized by a classical BAW resonator at 100MHz, "octar 507X100" from AR-Electronics. The oscillator near 1.6GHz clearly shows better performances than the one at 935MHz, with a noise level lower than -130dBc/Hz at 10kHz from the carrier. In order to compare the 100MHz oscillator with the 1.6GHz one, the low frequency source has to be multiplied by 16, *i.e.* +12dB must be added to the noise level. It gives a level of -140dBc/Hz at 10kHz which is not far from HBAR solution.

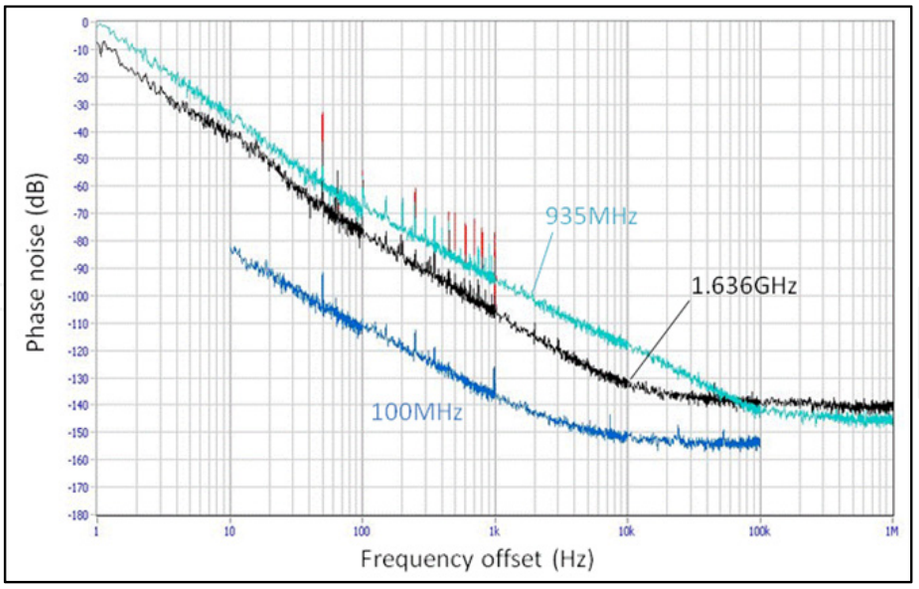

Figure 24. Phase noise curves for oscillators at 935MHz, 1,636MHz compared with phase noise of an oscillator stabilized by a classical BAW resonator at 100MHz [33].

6. Conclusions and perspectives

HBAR have been developed for the fabrication of passive radio-frequency devices capable to overcome standard SAW and BAW limitations considering the quality of the resonance, complexity of technological fabrication and operation frequencies.

These devices actually maximize the Q factor that can be obtained at room temperature using elastic waves, yielding quality factor times frequency products ($Q.f$) close or slightly above 10^{14}, *i.e.* effective Q factors of about 10,000 at 10GHz in theory (practically, Q factors in excess of 50,000 between 1.5 and 2GHz were experimentally achieved). Single-port or four-port resonator has been described and the different approach of manufacturing as been explained. The choice of acoustic wave and acoustic substrate permits to address large range of application. First one is chose value of the quality factor and the electromechanical coupling coefficient of overtone frequencies. Second one is to minimize frequency shift due to temperature variation for chosen frequency. All these possibilities allow us to address different applications such as sensor or low phase noise applications.

Although HBAR device knows since several decades, HBAR device has not yet achieve is development maturity. Futures works will concern improvement of fabrication, frequency control, and wireless sensors. The large number of the parameters for optimizing HBAR in function of the applications requires well-control generic process of fabrication. The selection of the frequency resonance is also a key point for the emergence of HBAR devices, as the frequency tuning. And finally, wireless HBAR sensor need strong effort of development.

Some simple applications and large potentiality of HBAR conception has been presented. Two main approaches exist for the realization of HBAR devices. The first one based on

piezoelectric deposition gives easily high quality factor and frequency device. The largest potentiality of conception to address different applications is obtained by the second approach based on mono-crystal wafer assembled. Further developments required to promote the industrial exploitation.

All previous technological industrial development for solidly mounted resonator for instance could be easily use for fabrication of HBAR based on piezoelectric deposition. More technological development is required to control thickness, repeatability and so on (see section 4.1) for the second approach. In both case, packaging aspect is a key-point. Both side of HBAR need to be free for acoustic reason. Flip-chip approach seems to give the best result for industrial needs.

In both cases, design tool needs to be developed to realize conception of all HBAR devices. SAW design tool could be a good base to develop such software.

More works also need to improve performances or to fixe limits of all different HBAR devices which are specialized for each application. These developments are the precondition for industrial actions.

Author details

T. Baron, E. Lebrasseur, F. Bassignot, G. Martin, V. Pétrini and S. Ballandras
FEMTO-ST, université de Franche-Comté, CNRS, ENSMM, UTBM, Département Temps-Fréquence, France

Acknowledgement

This work was partly supported by the Centre National d'Etudes Spatiales (CNES) under grant #04/CNES/1941/00-DCT094 and still supported by the CNES under grant #R-S08/TC-0001-026, and by the Direction Generale pour l'Armement (DGA) under grant #05.34.016.

7. References

[1] K. M. Lakin and J. S. Wang, UHF composite bulk wave resonators. *IEEE Ultrasonics Symposium Proceedings*, pp. 834-837, 1980

[2] K.M. Lakin, Thin film resonator technology. *IEEE Trans. on UFFC*, Vol.52, pp.707-716, 2005

[3] K.M. Lakin, G.R. Kline, K.T. McCarron, High Q microwave acoustic resonators and filters. *IEEE Trans. on Microwave Theory and Techniques, Vol. 41, n°12,* pp,2139-2146, 1993

[4] S.P. Caldwell, M.M. Driscoll, D. Stansberry, D.S. Bailey, H.L. Salvo, High overtone bulk acoustic resonator frequency stability improvements. *IEEE Trans. on FCS,* pp. 744-748, 1993

[5] D. Gachon, E. Courjon, G. Martin, L. Gauthier-Manuel, J.-C. Jeannot, W. Daniau and S. Ballandras, Fabrication of high frequency bulk acoustic wave resonator using thinned single-crystal Lithium Niobate layers. *Ferroelectrics, Vol. 362*, pp. 30-40, 2008

[6] Curran Daniel R & Al, US Patent #3401275A, 1968-09-10
[7] M. Pijolat, D. Mercier, A. Reinhardt, E. Defaÿ, C. Deguet, M. Aïd, J.S. Moulet, B. Ghyselen, S. Ballandras, Mode conversion in high overtone bulk acoustic wave resonators. *Proc. of the IEEE International Ultrasonics Symp.*, pp.201-204, 2008
[8] T. Baron, E. Lebrasseur, J.P. Romand, S. Alzuaga, S. Queste, G. Martin, D. Gachon, T. Laroche, S. Ballandras, J. Masson, Temperature compensated radio-frequency harmonic bulk acoustic resonators pressure sensors. *Proc. of the IEEE International Ultrasonics Symposium*, pp. 2040-2043, 2010.
[9] D. Gachon, T. Baron, G. Martin, E. Lebrasseur, E. Courjon, F. Bassignot, S. Ballandras, Laterally coupled narrow-band high overtone bulk wave filters using thinned single crystal lithium niobate layers. *Frequency Control and the European Frequency and Time Forum (FCS)*, 2011
[10] D. Royer & E. Dieulesaint. Elastic Waves in Solids II. *Springer*, 2000.
[11] R.A. Moore, J.T. Haynes, B.R. McAvoy. High Overtone Bulk Resonator Stabilized Microwave Sources. *1981 IEEE Ultrasonics Symposium*, pp.414-424, 1981
[12] B. Aspar, H. Moriceau, *et al.*. The generic nature of the Smart-Cut process for thin film transfer. *Journal of Electronic Materials*, Vol. 30, n°7, 2001, pp. 834-840
[13] T. Pastureaud, M. Solal, B. Biasse, B. Aspar, J.B. Briot, W. Daniau, W. Steichen, R. Lardat, V. Laude, A. Laëns, J.M. Frietd, S. Ballandras, High Frequency Surface Acoustic Waves Excited on Thin Oriented LiNbO3 Single Crystal Layers Transferred Onto Silicon. *IEEE Trans. on UFFC, Vol.54, n°4*, pp 870-876, 2007
[14] J.C. Ponçot, P. Nyeki, Ph. Defranould, J.P. Huignard. 3 GHz Bandwidth Bragg Cells. *IEEE 1987 Ultrasonics Symposium.* pp. 501-504, 1987
[15] T. Baron, E. Lebrasseur, *et al.*. Development of Composite Single Crystal Wafers for Sources and Sensor applications exploiting High-overtone Bulk Acoustic Resonators. *JNTE* 2010
[16] J.-S. Moulet, M. Pijolat, J. Dechamp, F. Mazen, A. Tauzin, F. Rieutord, A. Reinhardt, E. Defay, C. Deguet, B. Ghyselen, L. Clavelier, M. Aid, S. Ballandras, C. Mazure. High piezoelectric properties in LiNbO3 transferred layer by the Smart Cut™ technology for ultra wide band BAW filter applications. *Electron Devices Meeting, 2008. IEDM 2008. IEEE International.* pp. 1-4. 2008
[17] Hongyu Yu, Chuang-Yuan Lee, Wei Pang, Hao Zhang and Eun Sok Kim. Low Phase Noise, Low Power Consuming 3.7 GHz Oscillator Based on High-overtone Bulk Acoustic Resonator. *2007 IEEE Ultrasonics Symposium*, pp.1160-1163, 2007
[18] M. Pijolat, A. Reinhardt, *et al.*. Large Qxf Product for HBAR using Smart Cut (TM) transfer of LiNbO3 thin layers onto LiNbO3 substrate. *IEEE Ultrasonics Symposium 1-4 (2008)* pp. 201 – 204, 2008
[19] S. Ivanov, I. Koelyansky, G. Mansfeld and V. Veretin. Bulk Acoustic Wave High overtone resonator. *1990 1er congrès Français d'acoustique*, pp 599-601, 1990
[20] D. S. Bailey, M. M. Driscoll, and R. A. Jelen. Frequency Stability Of High Overtone Bulk Acous Tic Resonators. *1990 ultrasonics symposium.* pp. 509-512, 1990

[21] Lukas Baumgartel and Eun Sok Kim. Experimental Optimization of Electrodes for High Q, High Frequency HBAR. *2009 IEEE International Ultrasonics Symposium Proceedings.* pp. 2107-2110, 2009

[22] S.G.Alekseev, I.M.Kotelyanskii, G.D.Mansfeld, N.I.Polzikova. Energy Trapping in HBARs Based on Cubic Crystals. *2006 IEEE Ultrasonics Symposium*. pp. 1478-1480, 2006

[23] Hui Zhang, Zuoqing Wang, and Shu-Yi Zhang. Electrode Effects on Frequency Spectra and Electromechanical Coupling Factors of HBAR. *IEEE transactions on ultrasonics, ferroelectrics, and frequency control, vol. 52, no. 6*, june 2005

[24] Hui Zhang, Shu-Yi Zhang, Kai Zheng. Parameter characterization of high-overtone bulk acoustic resonators by resonant spectrum method. *Ultrasonics 43 (2005)* pp. 635–642. 2005

[25] J.J. Campbell, W.R. Jones, A method for estimating crystals cuts and propagation direction for excitation of piezoelectric surface waves. *IEEE Trans. On Sonics and Ultrasonics*, Vol. 15, pp. 209-217, 1968

[26] T. Baron, D. Gachon, *et al.*. Temperature Compensated Radio-Frequency Harmonic Bulk Acoustic Resonators. Proc of the IEEE IFCS, pp 625-655, 2010

[27] T. Baron, G. Martin, E. Lebrasseur, B. Francois, S. Ballandras, P.-P. Lasagne, A. Reinhardt, L. Chomeloux, D. Gachon, J.-M. Lesage. RF oscillators stabilized by temperature compensated HBARs based on LiNbO3/Quartz combination. *Frequency Control and the European Frequency and Time Forum (FCS), 2011 Joint Conference of the IEEE International.* pp. 1-4, 2011

[28] J.-M Friedt, C. Droit, G. Martin, and S. Ballandras, "A wireless interrogation system exploiting narrowband acoustic resonator for remote physical quantity measurement", *Rev. Sci. Instrum. vol. 81, 014701* (2010)

[29] C. Droit, G. Martin, S. Ballandras, J.-M Friedt, "A frequency modulated wireless interrogation system exploiting narrowband acoustic resonator for remote physical quantity measurement", *Rev. Sci Instrum. Vol 81, Issue 5, 056103* (2010)

[30] D. Rabus, G. Martin, E. Carry and S. Ballandras. Eight channel embedded electronic open loop interrogation for multi sensor measurements. *European Frequency and Time Forum (EFTF)*, 2012

[31] G.D. Mansfeld. THEORY OF HIGH OVERTONE BULK ACOUSTIC WAVE RESONATOR AS A GAS SENSOR. *13th International Conference on Microwaves, Radar and Wireless Communications.* vol.2, pp. 469 – 472, 2000

[32] Jérémy Masson. Étude de capteurs résonants acoustiques interrogeables à distance à base de films minces micro-usinés sur silicium. *Mémoire de thèse*, 2007

[33] E. Lebrasseur *et al.*. A Feedback-Loop Oscillator Stabilized Using Laterally-coupled-mode Narrow-band HBAR Filters. *2011 IEEE International Ultrasonics Symposium Proceedings,* 2011

[34] Hongyu Yu, Chuang-yuan Lee, Wei Pang, Hao Zhang, Alan Brannon, John Kitching, and Eun Sok Kim. HBAR-Based 3.6 GHz Oscillator with Low Power Consumption and Low Phase Noise. *IEEE Transactions on Ultrasonics, Ferroelectrics, and Frequency Control, vol. 56, no. 2, February 2009.* pp.400-403, 2009